Signatures of neutron star oscillations in post-glitch emission of radiopulsars

A.N. Timokhin

Sternberg Astronomical Institute, Moscow, Russia

Experimental study of NS structure

- Internal structure of celestial objects $\Longrightarrow$ need some kind of seismology
- In order to be able to proceed with seismological diagnostic two things are necessary:
  - Mechanism for oscillation excitation
  - Mechanism modulating radiation of the object

Observation of NS oscillations

- Neutron stars in binary systems:
  - Mechanism for oscillation excitation:
    instabilities in accretion flows.
  - Mechanism modulating radiation of the object:
    shaking of magnetic field lines, instabilities in boundary layer ...

  but, could we distinguish effects caused by oscillation of the *neutron star* and ones due to instabilities in the accretion flow? – which feature in the power spectrum corresponds to the *NS* oscillation and which to other processes?

- Isolated neutron stars – most of them radiopulsars:
  - Mechanism for oscillation excitation:
    glitch
  - Mechanism modulating radiation of the object:
    this work

Goldreich-Julian charge density and structure of the magnetosphere

Summary

- We consider NS as a conducting magnetized sphere on which surface an arbitrary velocity (vector) field is given. This field can be considered as a composition of series of Spheroidal and Toroidal modes with harmonic numbers (l, m).
- We looked for special configuration of electric field, such that, $\mathbf{E} \perp \mathbf{B}$ everywhere in the magnetosphere, so-called Goldreich-Julian field. Charge density in the magnetosphere, supporting such electric field $\rho_{GJ} \equiv \Delta \cdot \mathbf{E}/(4\pi)$is called Goldreich-Julian charge density.
- We derived equation for such field for for any oscillation mode (l, m) and analysed solutions of this equation.
- So, to some exted we generalized the pulsar “standard model” to the case of arbitrary oscillations. This allows us to study distortion of NS magnetosphere caused by star oscillations and estimate electromagnetic energy losses of an oscillating NS.

Assumptions

- We consider the near zone $r \ll 2\pi \frac{c}{\omega}$ where

$$\frac{1}{c}\partial_t \mathbf{E} \ll \nabla \times \mathbf{B}$$

- We assume that the physical current density in the magnetosphere is low enough – the magnetic field to first order in $\tilde{\xi} \equiv \xi / r_*$ can be considered as generated only by volume currents inside the NS and by surface currents on its surface, i.e.

$$\frac{4\pi}{c}\mathbf{j} \ll \nabla \times \mathbf{B}^{(1)} \sim \frac{l}{r}\left(B^{(0)}\frac{\xi}{r_*}\right)$$

- The latter implies

$$j \ll \frac{B\xi\omega l}{4\pi c r_*} c \, \frac{c}{r\omega} \simeq \rho_{GJ}(r_*) \, c \, \left(\frac{c}{\omega r}\right)$$

<BACK MENU

Basic Equations

- **Maxwell Equations**

$$\nabla \cdot \mathbf{E} = 4\pi\rho \quad (1)$$

$$\nabla \times \mathbf{E} = -\frac{1}{c}\partial_t \mathbf{B} \quad (2)$$

$$\nabla \cdot \mathbf{B} = 0 \quad (3)$$

$$\nabla \times \mathbf{B} = 0 \quad (4)$$

- **Boundary Conditions**

$$B_r(r_*) = B_{0r}$$

$$E_{\theta,\phi}(r_*) = -\frac{1}{c}(\mathbf{v}\times\mathbf{B}_0)_{\theta,\phi}$$

- **General Solution of the Maxwell equations**
  From (3), (4) it follows [Muslimov & Tsygan 1986]:

$$\mathbf{B} = \nabla\times\nabla\times(P\mathbf{e}_r)$$

  Substituting $\mathbf{B}$ into equation (2) we get

$$\mathbf{E} = -\frac{1}{c}\nabla\times(\partial_t P\mathbf{e}_r) - \nabla\Psi \qquad (5)$$

- **Equation for the electric field**
  We are looking for a charge density ρ_{GJ} yielding $\mathbf{E}\perp\mathbf{B}$

$$\mathbf{E}_{GJ}\cdot\mathbf{B} = 0 \qquad (6)$$

$$\rho_{GJ} = \frac{1}{4\pi}\nabla\cdot\mathbf{E}_{GJ} = -\frac{1}{4\pi}\Delta\Psi_{GJ} \qquad (7)$$

  substituting $\mathbf{E}$ from the expression for the general solution of Maxwell Equations (5) into equation (6) we get

Equation for the Goldreich-Julian potential Ψ_{GJ}

$$\Delta_\Omega P\, \partial_r \Psi_{GJ} - \partial_r \partial_\theta P\, \partial_\theta \Psi_{GJ} - \frac{1}{\sin^2\theta}\, \partial_r \partial_\phi P\, \partial_\phi \Psi_{GJ} + \\ + \frac{1}{c \sin\theta} \{\partial_r \partial_\phi P\, \partial_\theta \partial_t P - \partial_r \partial_\theta P\, \partial_\phi \partial_t P\} = 0 \tag{8}$$

$+$ **boundary conditions**

Equation for the Goldreich-Julian potential Ψ_{GJ}

$$\boxed{\Delta_\Omega P}\, \partial_r \Psi_{GJ} - \boxed{\partial_r \partial_\theta P}\, \partial_\theta \Psi_{GJ} - \frac{1}{\sin^2\theta} \boxed{\partial_r \partial_\phi P}\, \partial_\phi \Psi_{GJ} + \\ + \frac{1}{c \sin\theta} \left\{ \boxed{\partial_r \partial_\phi P}\, \partial_\theta \partial_t P - \boxed{\partial_r \partial_\theta P}\, \partial_\phi \partial_t P \right\} = 0 \qquad (8)$$

$+$ **boundary conditions**

- The terms in gray boxes are coefficients depending on the unperturbed magnetic field configuration, they do not depend on the concrete oscillation mode.

Equation for the Goldreich-Julian potential Ψ_{GJ}

$$\boxed{\Delta_\Omega P}\ \partial_r \Psi_{GJ} - \boxed{\partial_r \partial_\theta P}\ \partial_\theta \Psi_{GJ} - \frac{1}{\sin^2\theta} \boxed{\partial_r \partial_\phi P}\ \partial_\phi \Psi_{GJ} + \\ + \frac{1}{c \sin\theta} \left\{ \boxed{\partial_r \partial_\phi P}\ \boxed{\partial_\theta \partial_t P} - \boxed{\partial_r \partial_\theta P}\ \boxed{\partial_\phi \partial_t P} \right\} = 0 \qquad (8)$$

$+$ **boundary conditions**

- The terms in gray boxes are coefficients depending on the unperturbed magnetic field configuration, they do not depend on the concrete oscillation mode.
- Terms with $\partial_t P$ describe perturbations of the magnetic field by the stellar oscillations and are different for each oscillation mode (l, m).

Equation for the Goldreich-Julian potential Ψ_{GJ}

$$\boxed{\Delta_\Omega P}\ \partial_r \Psi_{GJ} - \boxed{\partial_r\partial_\theta P}\ \partial_\theta \Psi_{GJ} - \frac{1}{\sin^2\theta}\ \boxed{\partial_r\partial_\phi P}\ \partial_\phi \Psi_{GJ} +$$
$$+ \frac{1}{c\sin\theta}\left\{ \boxed{\partial_r\partial_\phi P}\ \boxed{\partial_\theta\partial_t P} - \boxed{\partial_r\partial_\theta P}\ \boxed{\partial_\phi\partial_t P} \right\} = 0 \qquad (8)$$

+ boundary conditions

- The terms in gray boxes are coefficients depending on the unperturbed magnetic field configuration, they do not depend on the concrete oscillation mode.
- Terms with $\partial_t P$ describe perturbations of the magnetic field by the stellar oscillations and are different for each oscillation mode (l, m).

This equation is linear PDE of the first order. Hence, oscillation modes can be considered separtely.

Rotation around z axis – Pulsar

- In this case the partial derivative ∂_t can be replaced by $-\Omega\,\partial_\phi$, where Ω is the angular velocity. Thus

$$\partial_t P = -\Omega\,\partial_\phi P$$

By direct substitution of

$$\Psi_{GJ} = -\frac{\Omega}{c}\sin\theta\,\partial_\theta P \tag{9}$$

it can be shown that the potential (9) is a solution of the equation (8) from the previous slide, and satisfies the boundary conditions for Ψ_{GJ}.

- For electric field and charge density we get

$$\begin{aligned}
\mathbf{E}_{GJ} &= -\frac{1}{c}(\boldsymbol{\Omega}\times\mathbf{r})\times\mathbf{B} \\
\rho_{GJ} &= -\frac{\boldsymbol{\Omega}\cdot\mathbf{B}}{2\pi c} + \frac{1}{4\pi c}(\boldsymbol{\Omega}\times\mathbf{r})\cdot(\nabla\times\mathbf{B})
\end{aligned}$$

Goldreich & Julian (1969), Mestel (1971)

Cosidered Cases

- Small amplitude oscillations of the NS with dipole magnetic field.
- Both **toroidal** ($\nabla \cdot \mathbf{V}_{osc} = 0$) and **spheroidal** ($\nabla \times \mathbf{V}_{osc} = 0$) oscillation modes were considered.
- Equation for Ψ_{GJ}can be solved analyticaly for both **toroidal** and **spheroidal** modes. Hence, Goldreich-Julian charge density can be calculated for any velocity field on the NS surface.
- **Examples**

  Spheroidal modes:

  Ψ_{GJ} (7,3); (7,2);

  ρ_{GJ} (7,3); (7,2);

  Toroidal modes:

  Ψ_{GJ} (1,0); (2,0); (2,1);

  ρ_{GJ} (1,0); (2,0); (2,1);

Distortion of the polar cap acceleration zone

Spheroidal Mode (44,4) and PSR J1824-2452

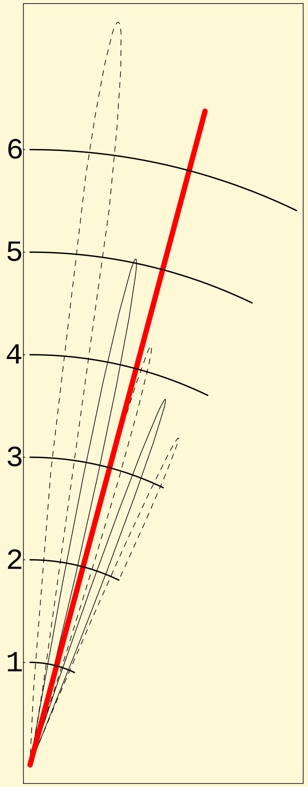

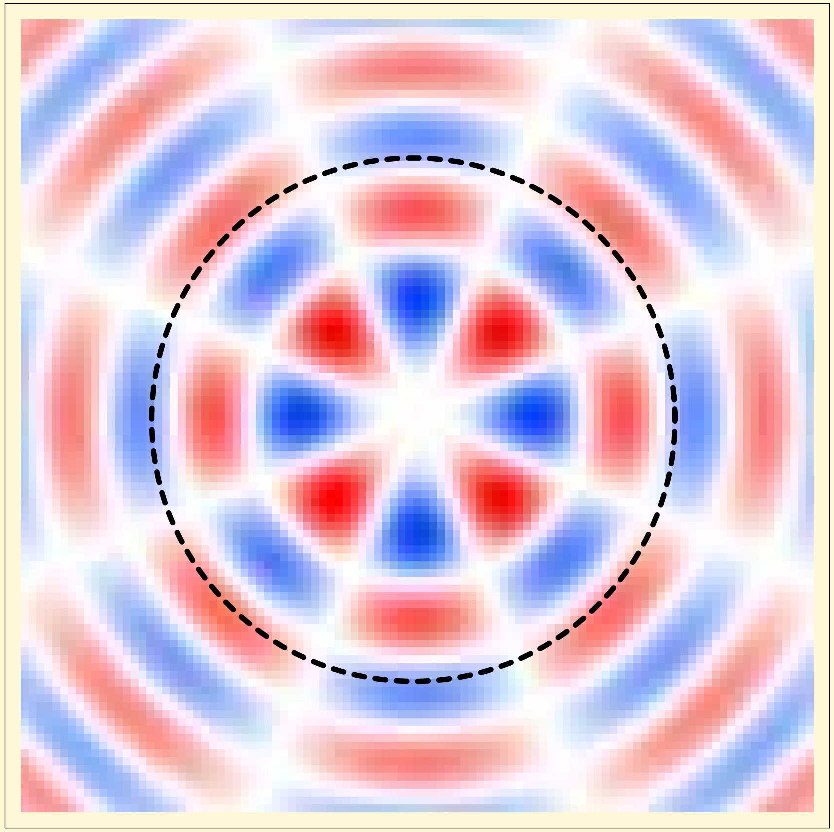

Figure 1: *left*: Goldreich-Julian Charge Density for oscillation mode $(44, 4)$ in polar coordinates $(\left|\rho_{GJ}^{lm}|_{r=r_*}\right|, \theta)$ for $\phi = 0$. The red line shows the angle at which the last closed fi eld line intersect the NS surface in PSR J1824-2452 (P=3.05 ms) *right*: The view of the PSR J1824-2452 polar cap (dashed circle). Goldreich-Julian Charge density for oscillation mode $(44, 4)$ is shown by the color map (red-positive, blue-negative)

GJ charge density: dependence on l

(24,4)

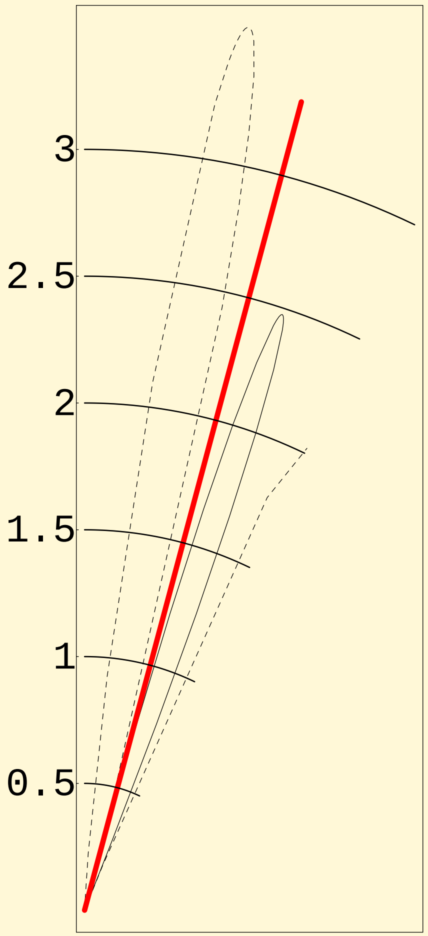

(44,4)

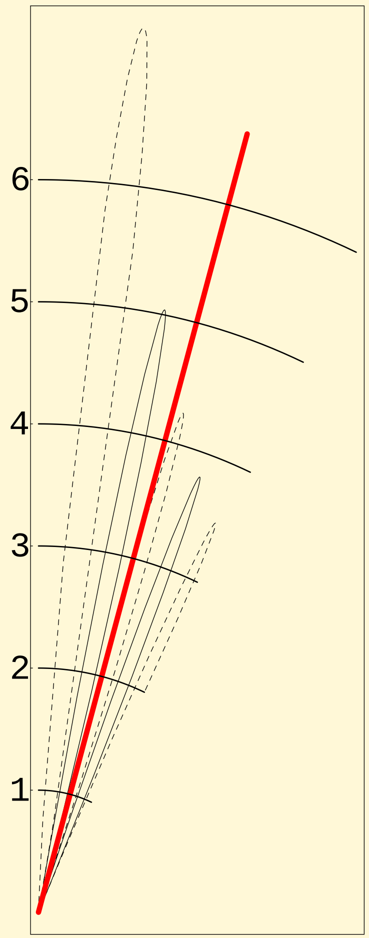

(64,4)

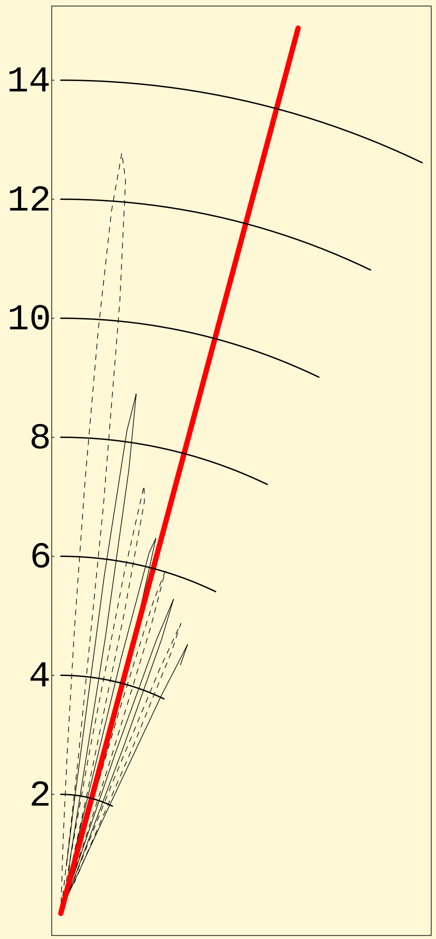

GJ charge density: dependence on m

(64,4)

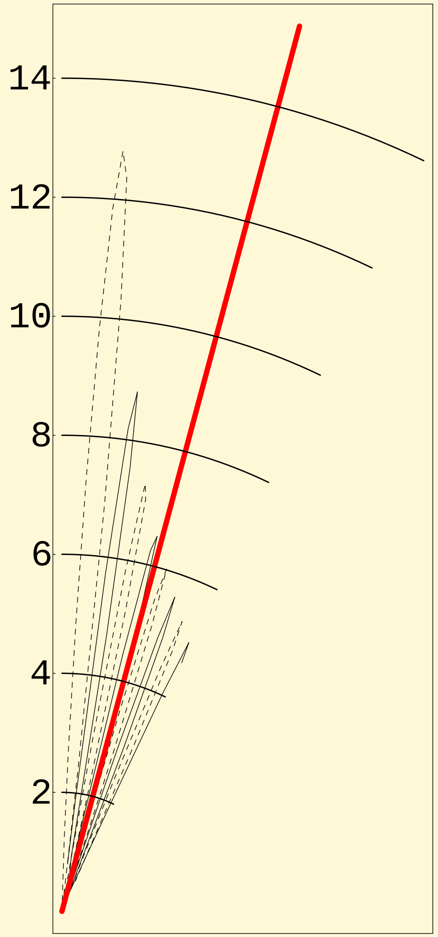

(64,8)

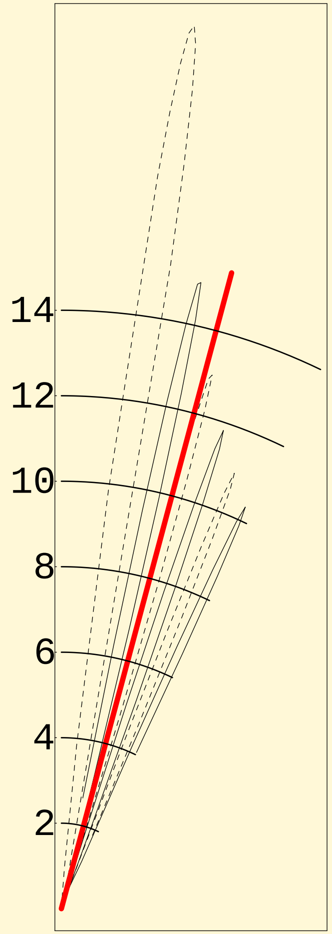

(64,14)

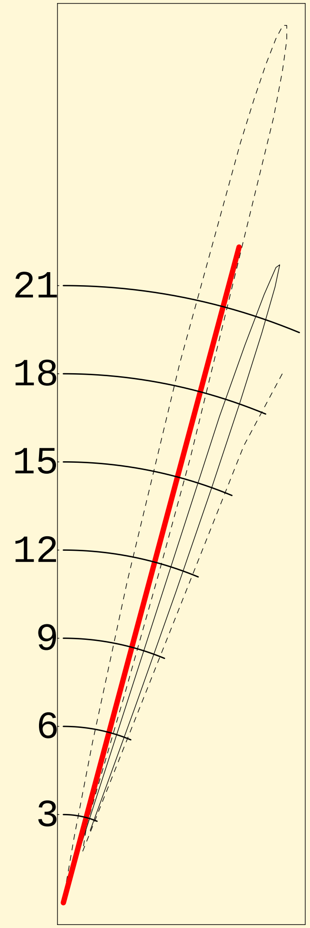

Oscillational GJ charge density

- The amplitude of ρ_{GJ} increases with increasing of the harmonic numbers l, m

  The reason:
  - the electric field

$$E \sim \frac{V_{osc}}{c} B$$

  - the charge density

$$\rho \sim \frac{E}{\delta x} \approx l \frac{E}{R}$$

- The amplitude of ρ_{GJ} for high harmonic numbers falls very rapidly with the distance from the NS

$E_{||}$ in the Polar Cap of pulsar for SCLF

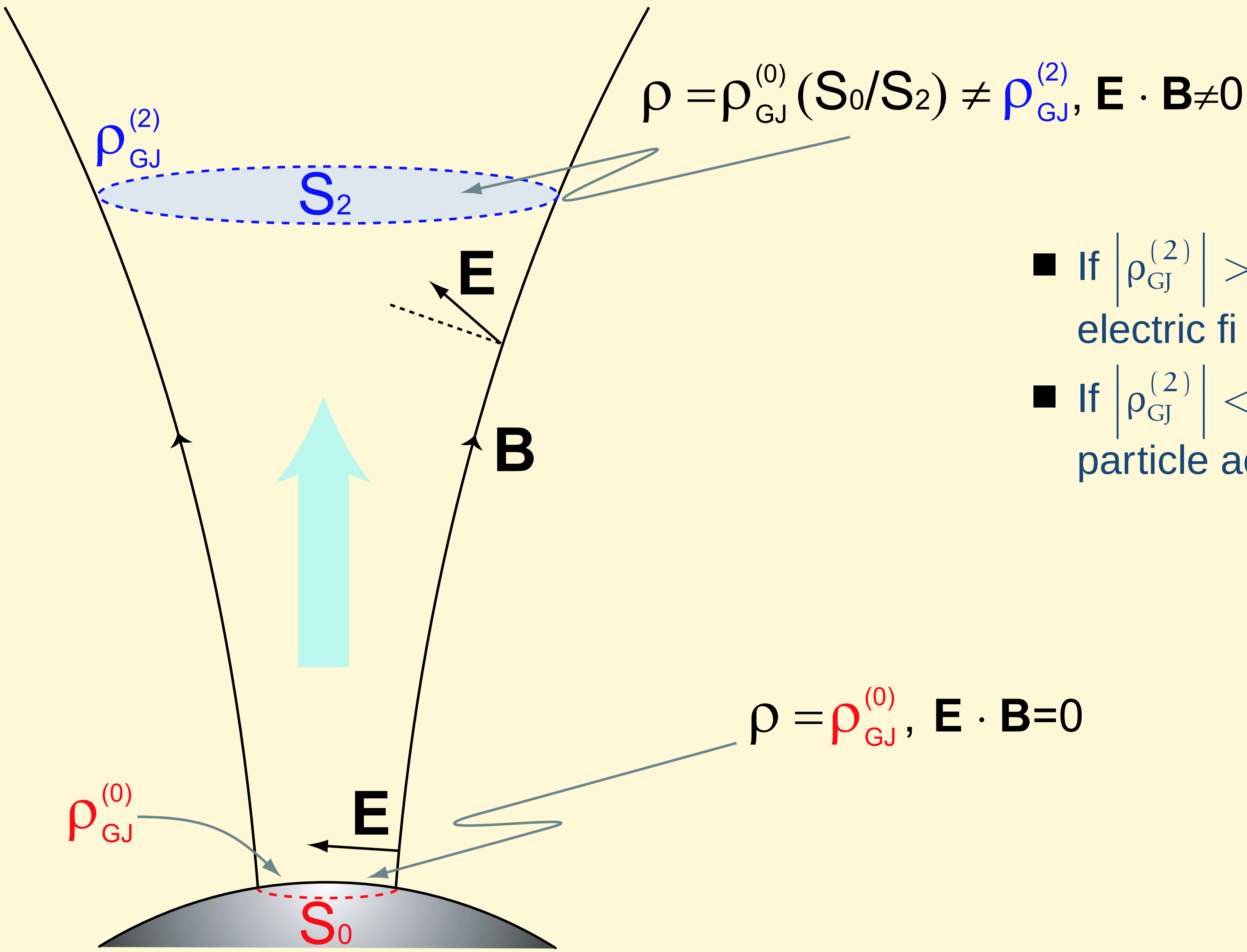

- If $\left|\rho_{GJ}^{(2)}\right| > |\rho|$ accelerating electric field is build
- If $\left|\rho_{GJ}^{(2)}\right| < |\rho|$ there will be no particle acceleration at all

Accelerating Potential: $\rho - \rho_{GJ}$ for $V_{rot} = V_{osc}$

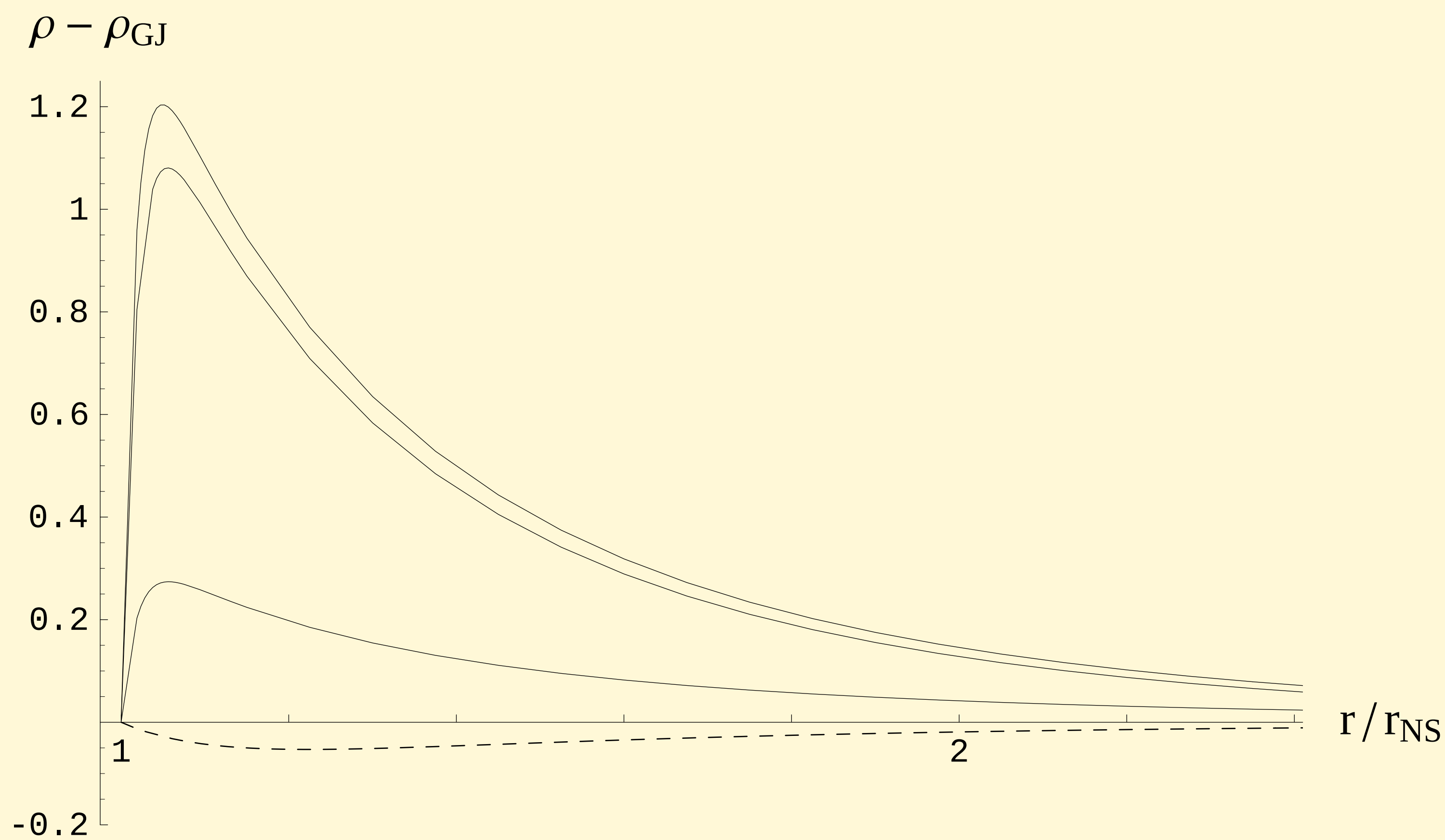

Figure 2: Difference between the charge density of space charge limited flow and the local Goldreich-Julian charge density along magnetic field lines in the polar cap region is shown (in arbitrary units) for three spheroidal modes with different (l, m): (64,14) – by the upper solid line, (54,14) – by the middle solid line, (54,2) – by the lower solid line. The same realtion for an aligned rotator is shown by the dashed line.

<BACK MENU

Velocity of oscillational motion

- Energy transferred during the glitch

$$W_{glitch} = I\Omega\Delta\Omega = I\Omega^2 \frac{\Delta\nu}{\nu} = i\ I_{NS}\left(\frac{2\pi}{P}\right)^2 \frac{\Delta\nu}{\nu}$$

- some fraction η of this energy goes to oscillation excitation

$$W_{osc} = \eta\ W_{glitch}$$

- Energy of oscillational motion

$$E_{osc} \simeq \frac{M_{osc}V_{osc}^2}{2} = \frac{\epsilon M_{NS}V_{osc}^2}{2}$$

- oscillational velocity

$$V_{osc} \simeq 500\ \eta_{\%}^{1/2}\ \epsilon^{-1/2}\ i^{1/2}\ P^{-1}\ \left(\frac{\Delta\nu}{\nu}\right)_6^{1/2} \mathrm{cm\ sec}^{-1}$$

Effective Goldreich-Julian charge density

- Electric fi eld induced by oscillations

$$E \simeq \frac{V_{osc}}{c} B$$

- Goldreich-Julian charge density for oscillational mode $(l, m) \sim \mathbf{1}$

$$\rho_{GJ}^{osc} \sim \frac{E}{\Delta x} \simeq \mathbf{1} \frac{E}{r_*} = \mathbf{1} \frac{V_{osc}}{c} \frac{B}{r_*}$$

- Efective Goldreich-Julian charge density
  - oscillational

$$\rho_{GJ}^{osc,eff} \sim \rho_{GJ}^{osc}$$

  - rotational – Muslimov & Tsygan model (particles freely escape NS surface)

$$\rho_{GJ}^{rot,eff} \sim \kappa \rho_{GJ}^{rot} \simeq .15 \; \rho_{GJ}^{rot}$$

  - rotational – Ruderman & Sutherland model (particles do not escape NS surface)

$$\rho_{GJ}^{rot,eff} \sim \rho_{GJ}^{rot}$$

Distortion of the accelerating electric field

Distortion of the accelerating electric fi eld in the polar cap is proportional to

$$\frac{\rho_{\rm GJ}^{\rm osc,eff}}{\rho_{\rm GJ}^{\rm rot,eff}}$$

- for Muslimov & Tsygan model

$$\frac{\rho_{\rm GJ}^{\rm osc,eff}}{\rho_{\rm GJ}^{\rm rot,eff}} \simeq 3.5 \times 10^{-3}\ \mathbf{1}\ \eta_{\%}^{1/2}\ \epsilon^{-1/2}\ i^{1/2}\ \left(\frac{\Delta\nu}{\nu}\right)_6^{1/2}$$

- Ruderman & Sutherland model

$$\frac{\rho_{\rm GJ}^{\rm osc,eff}}{\rho_{\rm GJ}^{\rm rot,eff}} \simeq 5.3 \times 10^{-4}\ \mathbf{1}\ \eta_{\%}^{1/2}\ \epsilon^{-1/2}\ i^{1/2}\ \left(\frac{\Delta\nu}{\nu}\right)_6^{1/2}$$

Harmonics where acceleration is damped

When $\frac{\rho_{GJ}^{osc,eff}}{\rho_{GJ}^{rot,eff}} \sim 1$ accleration of particles in the polar cap will be blocked periodically. This occurs

- for Muslimov & Tsygan model, when

$$\mathbf{1} > 300\ \eta_{\%}^{-1/2}\ \epsilon^{1/2}\ i^{-1/2}\ \left(\frac{\Delta\nu}{\nu}\right)_6^{-1/2}$$

- Ruderman & Sutherland model, when

$$\mathbf{1} > 2000\ \eta_{\%}^{-1/2}\ \epsilon^{1/2}\ i^{-1/2}\ \left(\frac{\Delta\nu}{\nu}\right)_6^{-1/2}$$

<BACK MENU

Possible observational signatures

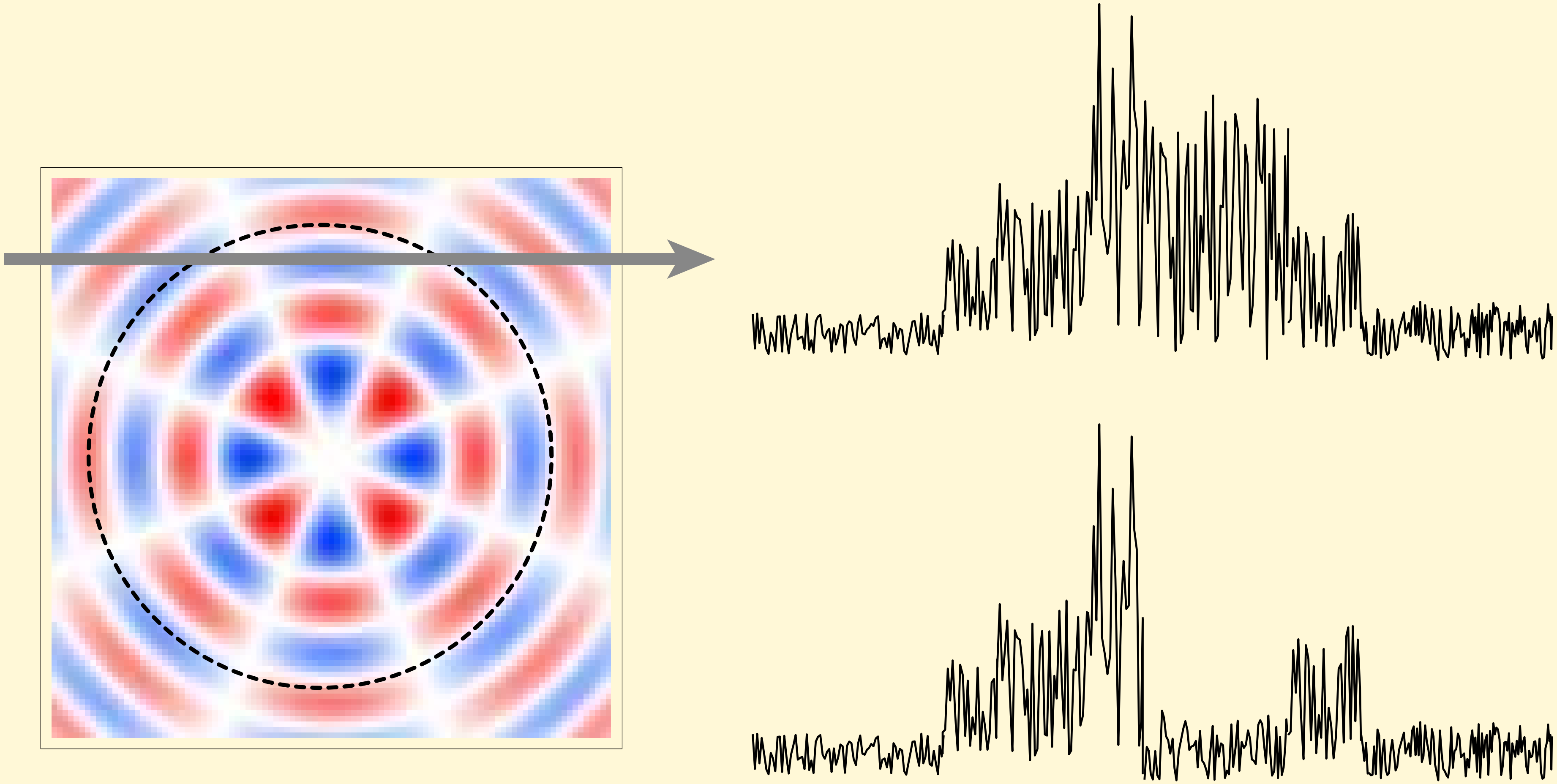

Figure 3: Schematic view of individual pulse distortion in pulsar due to oscillation of the netron star.

Conclusions

- For the half of oscillation modes a strong current ($\gg \rho_{GJ}c$) will flow along *closed* magnetic field lines
- In the polar cap region particle acceleration rate could be modulated with oscillation period. For oscillation modes with l, m large enough "decelerating" electric field could be of compatible strength with the accelerating field due to pulsar rotation even if $V_{osc} << V_{rot} = \Omega r_*$

- Region of closed field lines could become visible
- Oscillations can distort acceleration of particles in the polar cap region of the pulsar and change its radiation pattern
- Distortion of the geometry of radiation region due to shaking of magnetic field lines is also possible, but is much more difficult to observe

Boundary Conditions

- **Magnetic field**

  $\mathbf{B} = \nabla\times\nabla\times P\mathbf{e}_r\,,$ to the first order in $\frac{\xi}{r}$: $P \approx P_0(r,\theta,\phi) + \delta P(t,r,\theta,\phi)$

$$\partial_t\,\delta P = \sum_{l,m}\left(\frac{r_*}{r}\right)^l \partial_t\,\delta p_{lm}(t)\,Y_{lm}(\theta,\phi)$$

$$\partial_t\,\delta p_{lm}(t) = \frac{1}{l(l+1)}\int_{4\pi} d\Omega\,Y^*_{lm}\{\mathbf{v}\cdot\nabla(\Delta_\Omega P_0)+ \\ +\Delta_\Omega P_0\,(\nabla\cdot\mathbf{v}_\perp) + r^2(\nabla_\perp(\partial_r P_0)\cdot\nabla_\perp)\,v_r\}\Big|_{r=r_*}$$

- **Boundary Conditions for Ψ_{GJ}**

$$\Psi_{GJ}|_{r=r_*} = -\frac{1}{c}\int\left\{\frac{1}{r}\Delta_\Omega P_0\,v_\phi + \frac{1}{\sin\theta}\partial_r\partial_\phi P_0\,v_r + \frac{1}{\sin\theta}\partial_\phi\partial_t\,\delta P\right\}d\theta\Big|_{r=r_*} + e^{-i\omega t}F(\phi)$$

$$\Psi_{GJ}|_{\theta=0;\;r=r_*} = 0$$

Oscillation modes

- The oscillation velocity components for spheroidal ($\nabla \times \boldsymbol{v} = 0$) oscillations are

$$v_r = e^{-i\omega t}\, U(r)\, Y_{lm}(\theta,\phi), \quad v_\theta = e^{-i\omega t}\, V(r)\, \partial_\theta Y_{lm}(\theta,\phi),$$
$$v_\phi = e^{-i\omega t}\, V(r)\, \frac{1}{\sin\theta}\partial_\phi Y_{lm}(\theta,\phi)$$

where U and V are radial and transversal velocity amplitude respectively.

- The oscillation velocity components for toroidal ($\nabla \cdot \boldsymbol{v} = 0$) oscillations are

$$v_r = 0, \quad v_\theta = e^{-i\omega t}\, W(r)\, \frac{1}{\sin\theta}\partial_\phi Y_{lm}(\theta,\phi), \quad v_\phi = -e^{-i\omega t}\, W(r)\, \partial_\theta Y_{lm}(\theta,\phi)$$

where W is transversal velocity amplitude.

Toroidal Oscillations

- Equation for Ψ_{GJ}

$$2\cos\theta\ \partial_r\Psi_{GJ}^{lm} + \frac{1}{r}\sin\theta\ \partial_\theta\Psi_{GJ}^{lm} - \frac{m^2}{l(l+1)}\frac{B_0 w}{c}\left(\frac{r_*}{r}\right)^{l+1} Y_{lm} = 0$$

- Boundary conditions

$$\Psi_{GJ}^{lm}|_{r=r_*} = -\frac{B_0 w r_*}{c}\int\left(\cos\theta\,\partial_\theta Y_{lm} - \frac{m^2}{l(l+1)}\frac{Y_{lm}}{\sin\theta}\right)d\theta + e^{-i\omega t}\,F(\phi)\,,$$

$$\Psi_{GJ}^{lm}|_{\theta=0,r=r_*} = 0\,.$$

- Solution

$$\Psi_{GJ}^{lm} = \frac{m^2}{l(l+1)}\frac{B_0 W r_*}{c}\left(\frac{r_*}{r}\right)^{l}\sin^{2l}\theta\int\frac{Y_{lm}}{(\sin\theta)^{2l+1}}\,d\theta + \Phi_{lm}\left(\sin\theta\left(\frac{r_*}{r}\right)^{1/2},\phi,t\right)$$

Spheroidal oscillations

- Equation for Ψ_{GJ}

$$2\cos\theta\,\partial_r\Psi_{GJ}^{lm} + \frac{1}{r}\sin\theta\,\partial_\theta\Psi_{GJ}^{lm} - \frac{B_0}{c}\left[Z_1\left(\frac{r_*}{r}\right)^l\partial_\phi Y_{l-1}^m + Z_2\left(\frac{r_*}{r}\right)^{l+2}\partial_\phi Y_{l+1}^m\right] = 0\,,$$

where

$$Z_1 = \frac{1}{l}((l+1)V - U/2)\sqrt{\frac{l^2-m^2}{4l^2-1}} \qquad Z_2 = \frac{1}{l+1}(lV + U/2)\sqrt{\frac{(l+1)^2-m^2}{(2l+3)(2l+1)}}$$

- Boundary conditions

$$\Psi_{GJ}^{lm}|_{r=r_*} = -\frac{B_0 r_*}{c}\int\left(V\cot\theta\,\partial_\phi Y_{lm} - Z_1\frac{\partial_\phi Y_{l-1}^m}{\sin\theta} - Z_2\frac{\partial_\phi Y_{l+1}^m}{\sin\theta} - \right)d\theta + e^{-i\omega t}F(\phi)\,,$$

$$\Psi_{GJ}^{lm}|_{\theta=0,r=r_*} = 0$$

- Solution

$$\Psi_{GJ}^{lm} = -\frac{B_0 r_*}{c}\left\{Z_1\left(\frac{r_*}{r}\right)^{l-1}(\sin\theta)^{2l-2}\int\frac{\partial_\phi Y_{l-1}^m}{(\sin\theta)^{2l-1}}d\theta + Z_2\left(\frac{r_*}{r}\right)^{l+1}(\sin\theta)^{2l+2}\int\frac{\partial_\phi Y_{l+1}^m}{(\sin\theta)^{2l+3}}d\theta\right\} + \Phi_{lm}\left(\sin\theta\left(\frac{r_*}{r}\right)^{1/2},\phi,t\right)$$

Spheroidal mode (7,3)

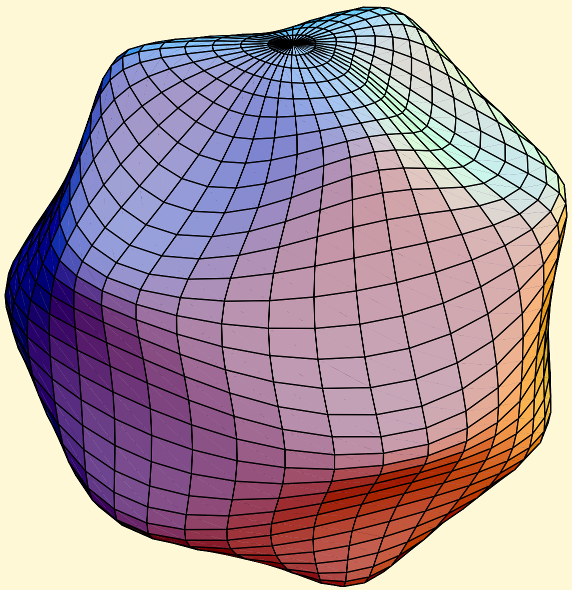

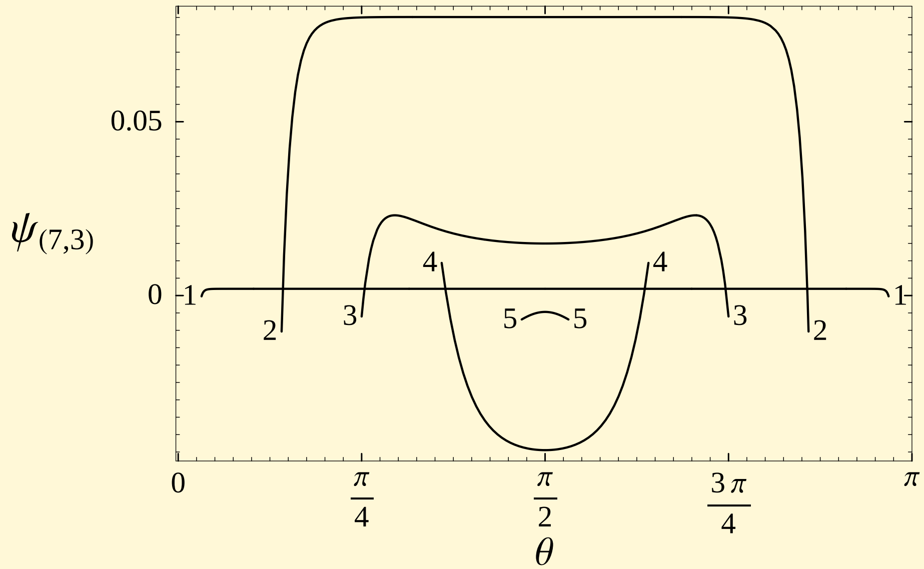

Figure 4: *left*: Deformation of the star surface during oscillation in spheroidal mode $(7,3)$ *right*: The potential Ψ_{GJ}^{73} along a dipolar magnetic fi eld line as a function of the polar angle θ is shown for 5 fi eld lines with azimuthal angle $\phi = 0$ at $t = 2\pi n/\omega$.

Spheroidal mode (7,3): GJ charge density

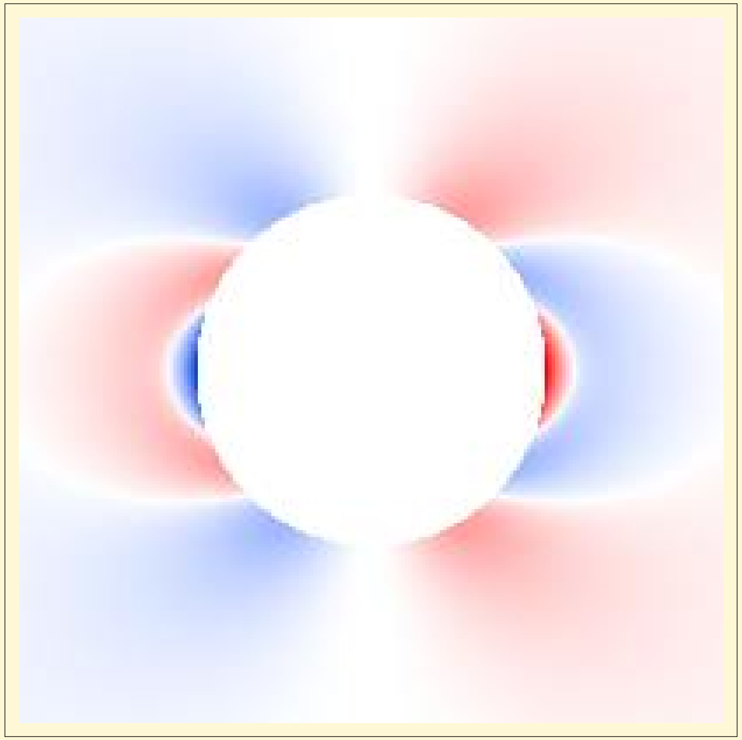

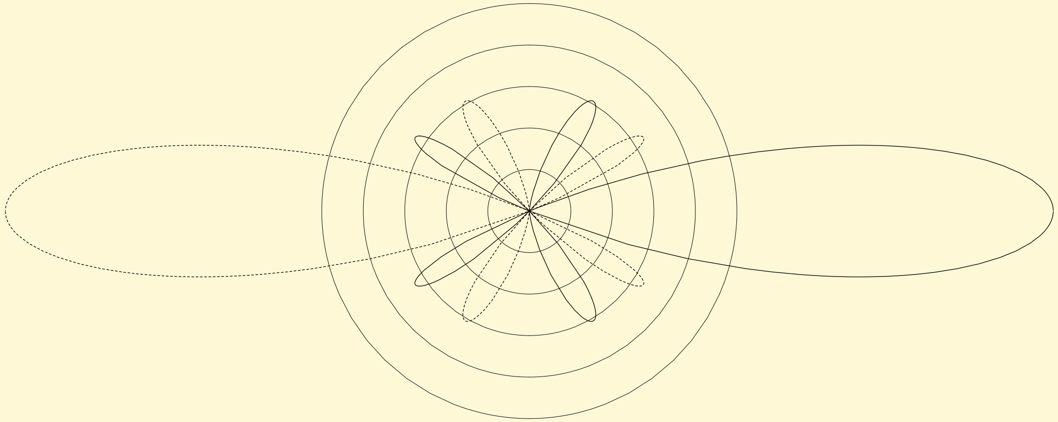

Figure 5: *left*: The charge density ρ_{GJ}^{73} near the NS for azimuthal angle $\phi = 0$ at $t = 2\pi n/\omega$. Positive values of charge density are shown by red and negative ones by blue color. *right*: The charge density $\rho_{GJ}^{73}|_{r=r_*}$ on the NS surface is shown in a polar coordinate system $(\left|\rho_{GJ}^{lm}|_{r=r_*}\right|, \theta)$ for $\phi = 0$. Positive values of charge density are shown by the solid line and negative ones by the dashed line.

Spheroidal mode (7,2)

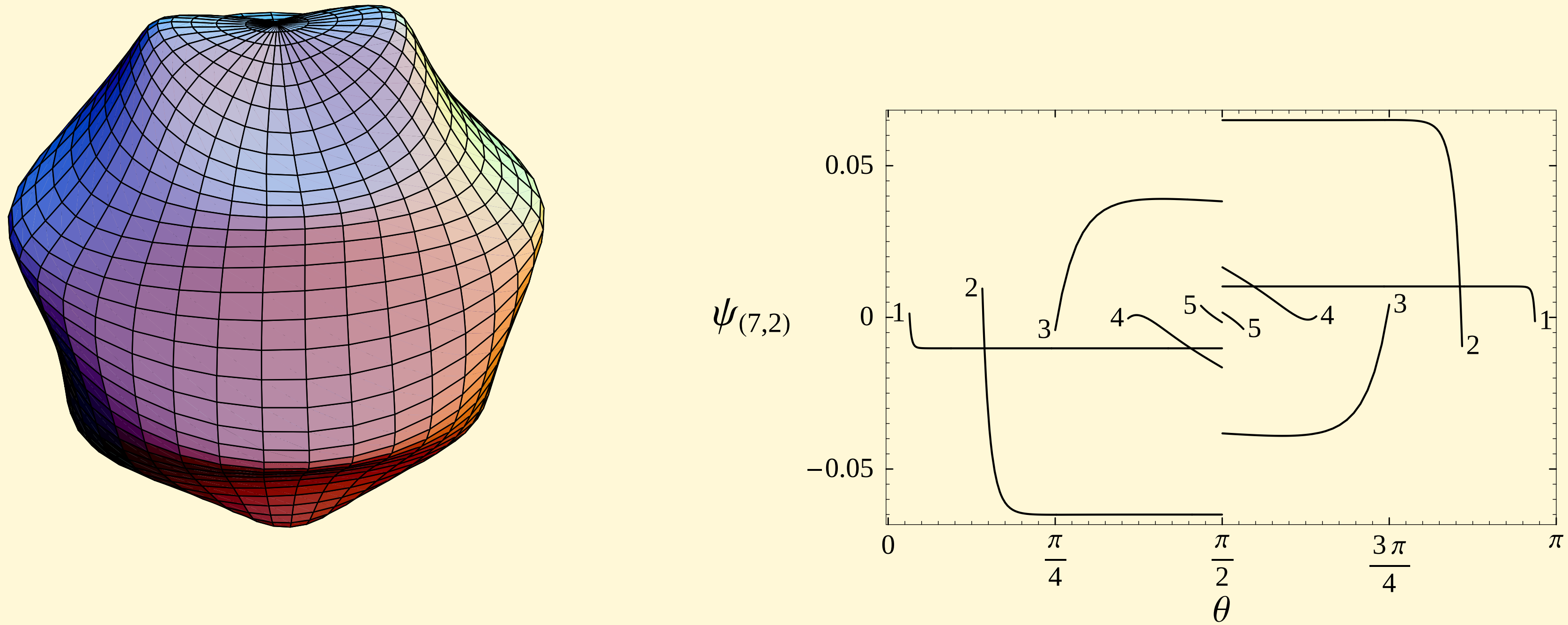

Figure 6: *left*: Deformation of the star surface during oscillation in spheroidal mode $(7,2)$ *right*: The potential Ψ_{GJ}^{72} along a dipolar magnetic fi eld line as a function of the polar angle θ is shown for 5 fi eld lines with azimuthal angle $\phi = 0$ at $t = 2\pi n/\omega$.

Spheroidal mode (7,2): GJ charge density

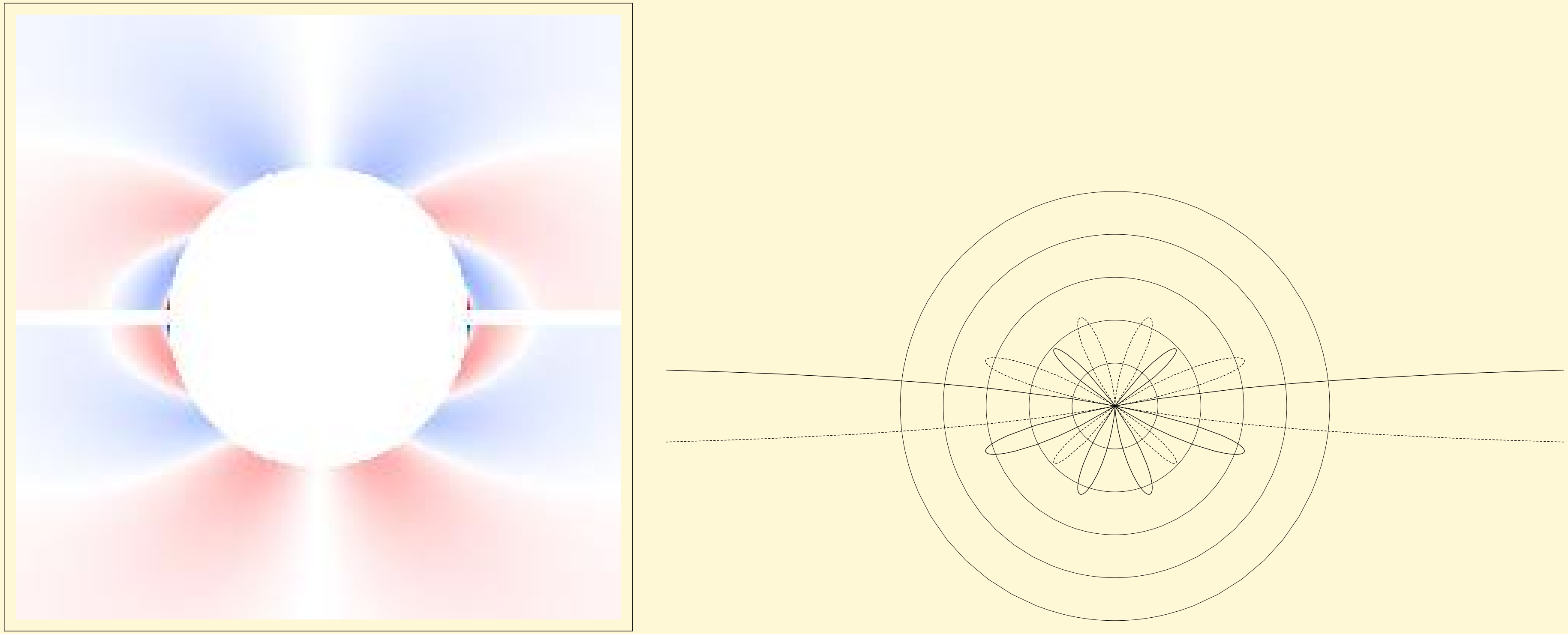

Figure 7: *left*: The charge density ρ_{GJ}^{72} near the NS for azimuthal angle $\phi = 0$ at $t = 2\pi n/\omega$. Positive values of charge density are shown by red and negative ones by blue color. *right*: The charge density $\rho_{GJ}^{72}|_{r=r_*}$ on the NS surface is shown in a polar coordinate system $\left(\left|\rho_{GJ}^{lm}|_{r=r_*}\right|, \theta\right)$ for $\phi = 0$. Positive values of charge density are shown by the solid line and negative ones by the dashed line. NB: on the equatorial plane ($\theta = \pi/2$) ρ_{GJ}^{72} is infi nite.

Toroidal mode (1,0)

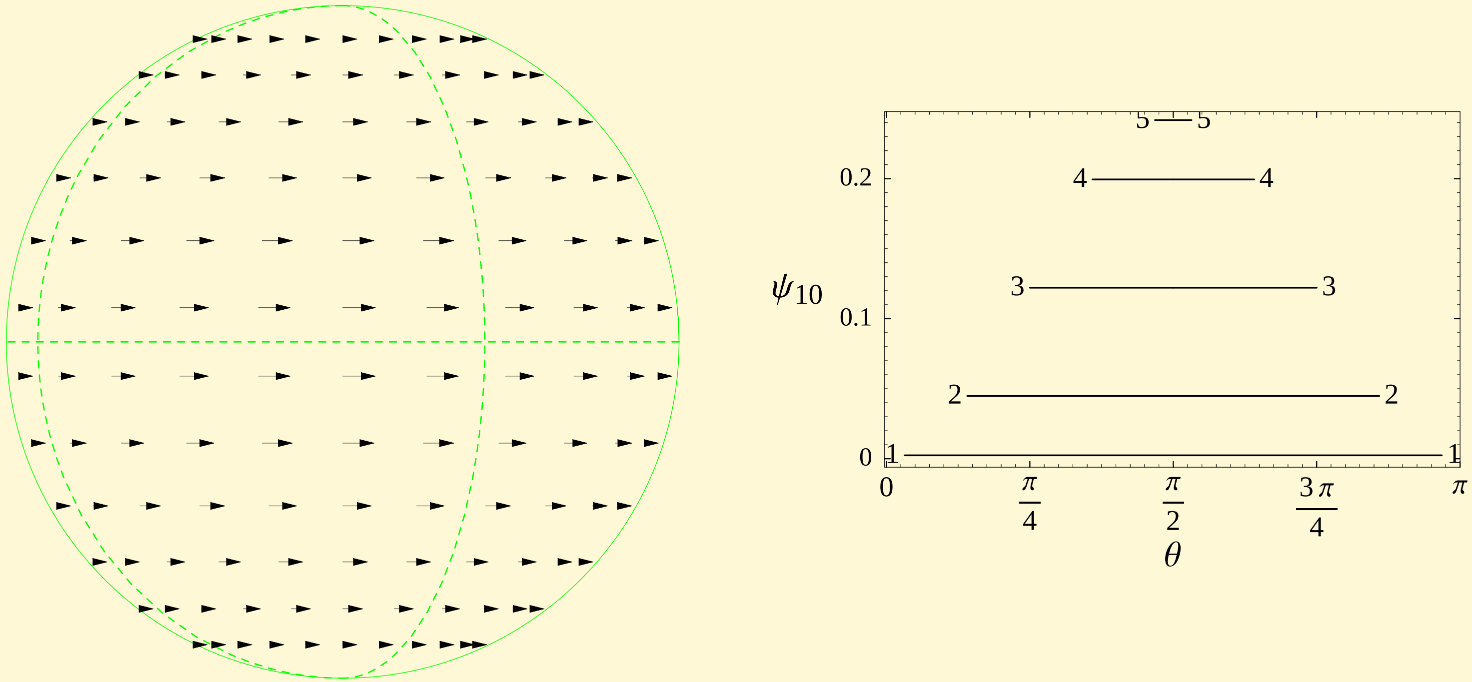

Figure 8: *left*: Velocity field on a sphere for the toroidal mode $(1, 0)$ is shown at the time $t = 2\pi n/\omega$, where n is an integer, as projection on the meridional plane $\phi = -115°$. *right*: The potential Ψ_{GJ}^{10} along a dipolar magnetic field line as a function of the polar angle θ is shown for 5 field lines for $t = 2\pi n/\omega$. NB: aligned rotator

Toroidal mode (1,0): GJ charge density

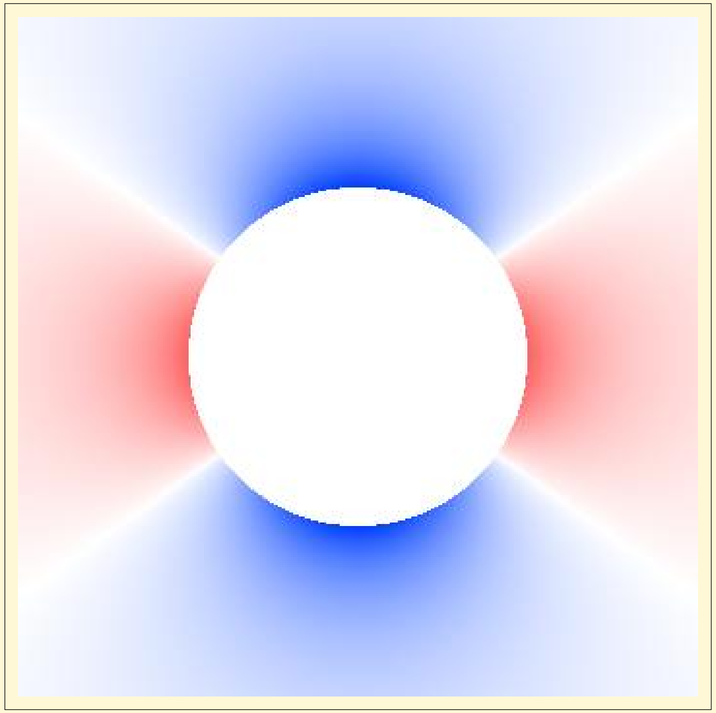

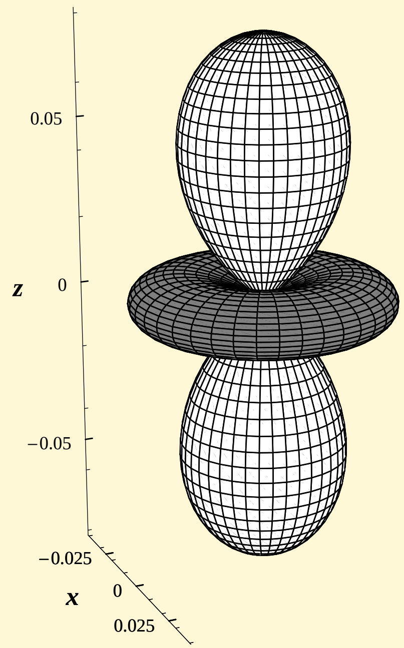

Figure 9: *left*: The charge density $\rho_{\rm GJ}^{10}$ near the NS at $t = 2\pi n/\omega$. Positive values of charge density are shown by red and negative ones by blue color. *right*: The charge density $\rho_{\rm GJ}^{10}|_{r=r_*}$ on the NS surface is shown in a spherical coordinate system $\left(\left|\rho_{\rm GJ}^{lm}|_{r=r_*}\right|, \theta, \phi\right)$. Positive values of charge density are shown by a gray surface and negative ones by white. NB: aligned rotator

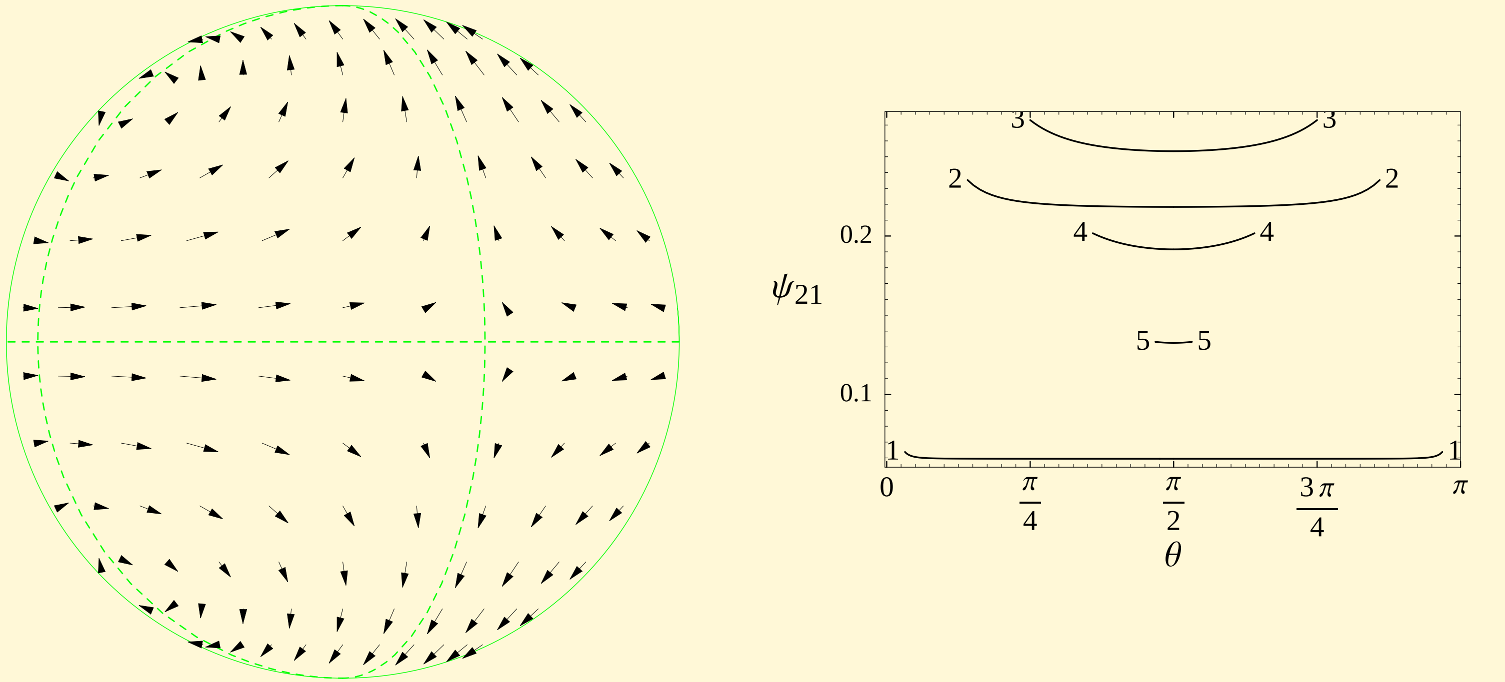

Figure 10: *left*: Velocity field on a sphere for the toroidal mode $(2,1)$ is shown at the time $t = 2\pi n/\omega$, where n is an integer, as projection on the meridional plane $\phi = -115°$. *right*: The potential Ψ_{GJ}^{21} along a dipolar magnetic field line as a function of the polar angle θ is shown for 5 field lines with azimuthal angle $\phi = \pi/2$ at $t = 2\pi n/\omega$.

Toroidal mode (2,1): GJ charge density

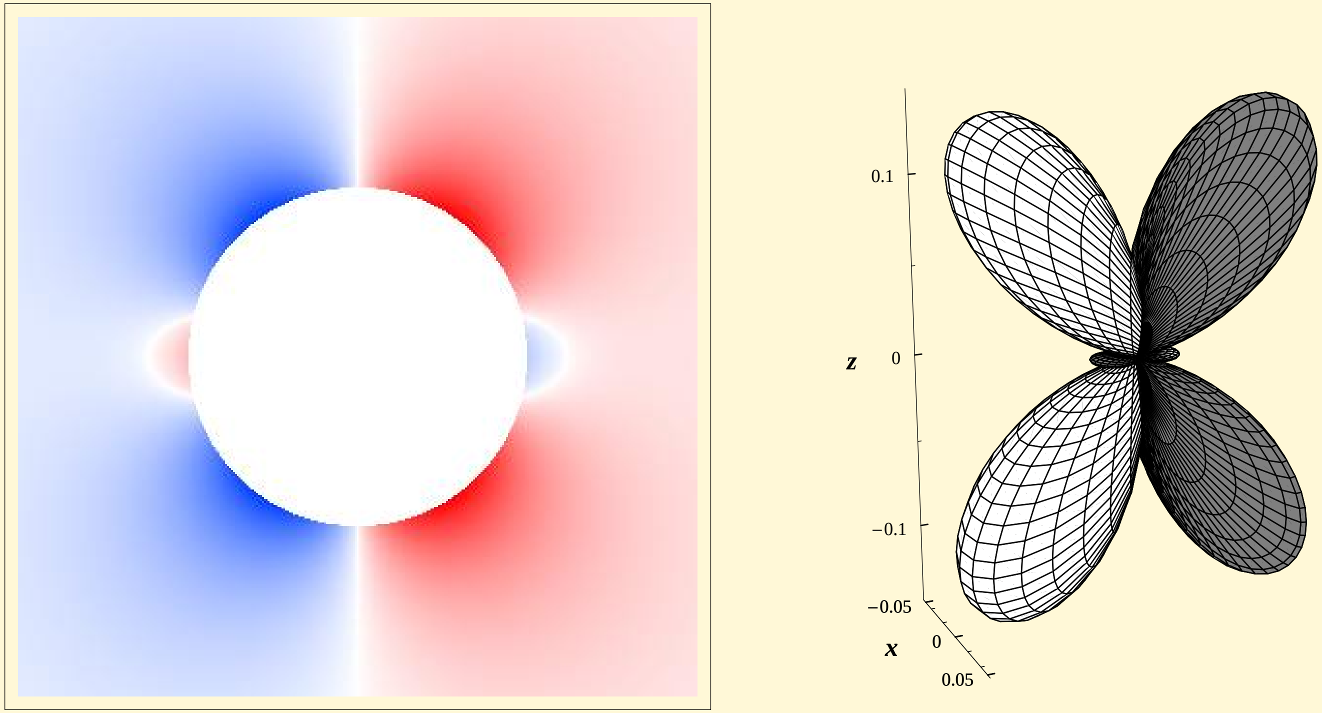

Figure 11: *left*: The charge density ρ_{GJ}^{21} near the NS for azimuthal angle $\phi = \pi/2$ at $t = 2\pi n/\omega$. Positive values of charge density are shown by red and negative ones by blue color. *right*: The charge density $\rho_{GJ}^{21}|_{r=r_*}$ on the NS surface is shown in a spherical coordinate system $(\left|\rho_{GJ}^{lm}|_{r=r_*}\right|, \theta, \phi)$. Positive values of charge density are shown by a gray surface and negative ones by white.

Toroidal mode (2,0)

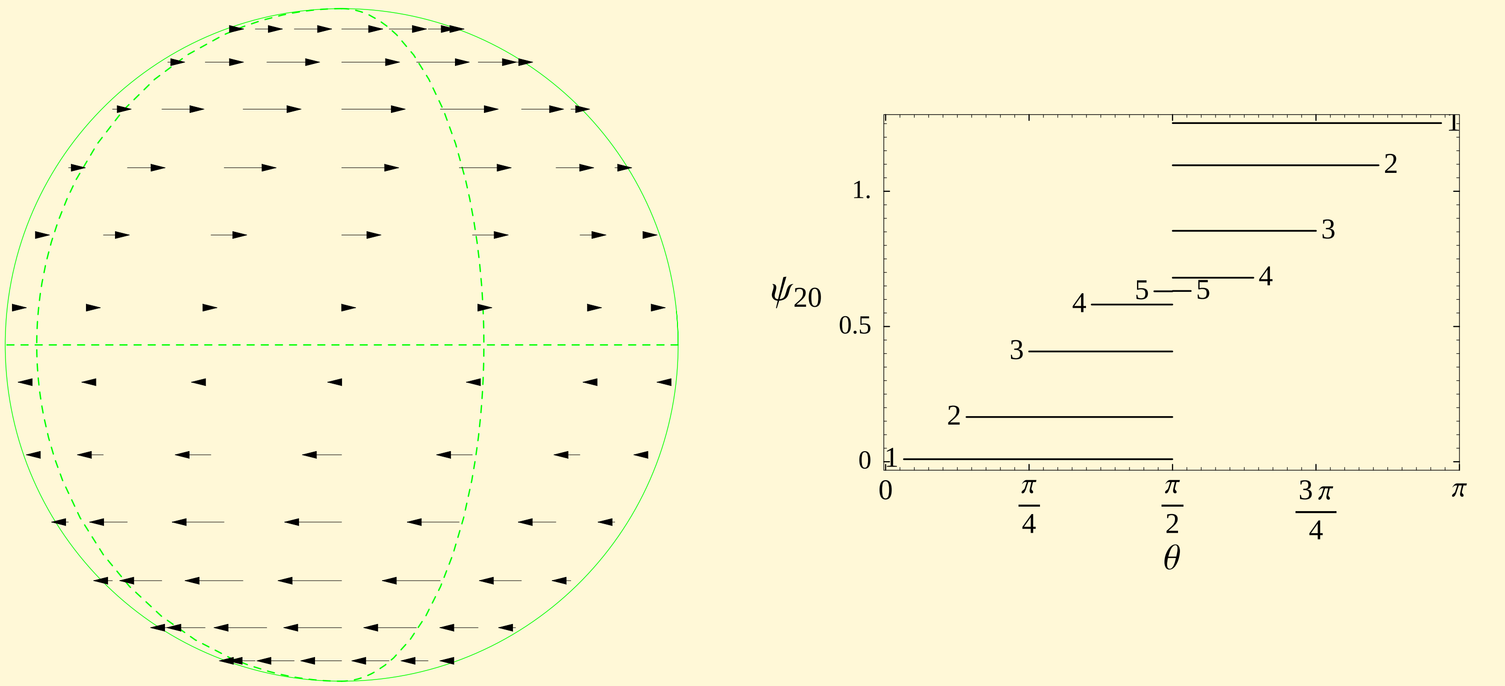

Figure 12: *left*: Velocity field on a sphere for the toroidal mode $(2,0)$ is shown at the time $t = 2\pi n/\omega$, where n is an integer, as projection on the meridional plane $\phi = -115^\circ$. *right*: The potential Ψ_{GJ}^{20} along a dipolar magnetic field line as a function of the polar angle θ is shown for 5 field lines at $t = 2\pi n/\omega$.

Toroidal mode (2,0): GJ charge density

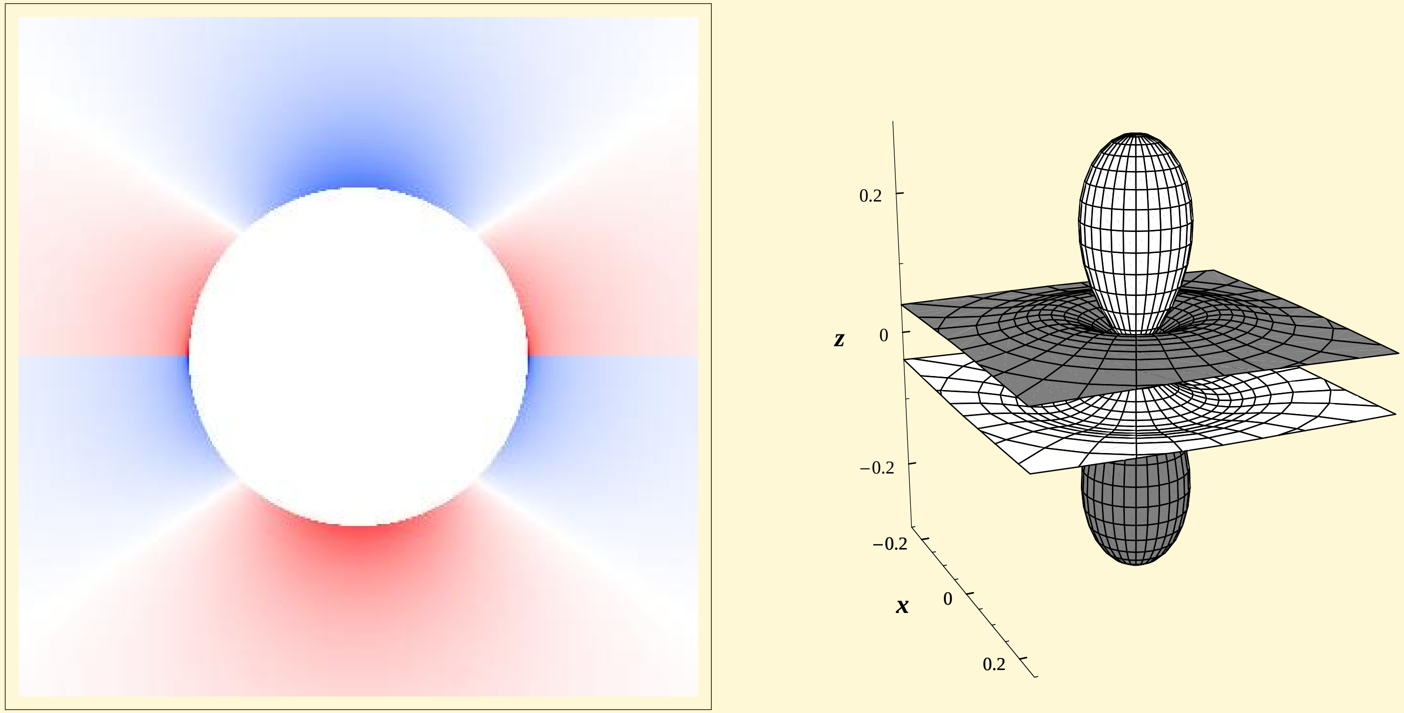

Figure 13: *left*: The charge density $\rho_{\rm GJ}^{20}$ near the NS at $t = 2\pi n/\omega$. Positive values of charge density are shown by red and negative ones by blue color. *right*: The charge density $\rho_{\rm GJ}^{20}|_{r=r_*}$ on the NS surface is shown in a spherical coordinate system $\left(\left|\rho_{\rm GJ}^{lm}|_{r=r_*}\right|, \theta, \phi\right)$. Positive values of charge density are shown by the gray surface and negative ones by the white. **NB: on the equatorial plane ($\theta = \pi/2$) $\rho_{\rm GJ}^{20}$ is infinite** .

Strong current in the magnetosphere

- For toroidal modes with even $(l - m)$, and spheroidal modes with odd $(l - m)$ the strong current with the current density

$$\rho_{\mathrm{GJ}}(r_*)\, c\, \left(\frac{c}{\omega r}\right)$$

should flow along closed magnetic field lines.

- For the open magnetic field lines we could use our solution

Strong current in the magnetosphere

- For toroidal modes with even $(l - m)$, and spheroidal modes with odd $(l - m)$ the strong current with the current density

$$\rho_{\text{GJ}}(r_*)\ c\ \left(\frac{c}{\omega r}\right)$$

should flow along closed magnetic field lines.

- For the open magnetic field lines we could use our solution

Observational manifestations

- This current could generate plasma instabilities and make closed field line regions visible.
- Oscillation modes generating strong current will be more effectively damped.

Glitching Pulsars

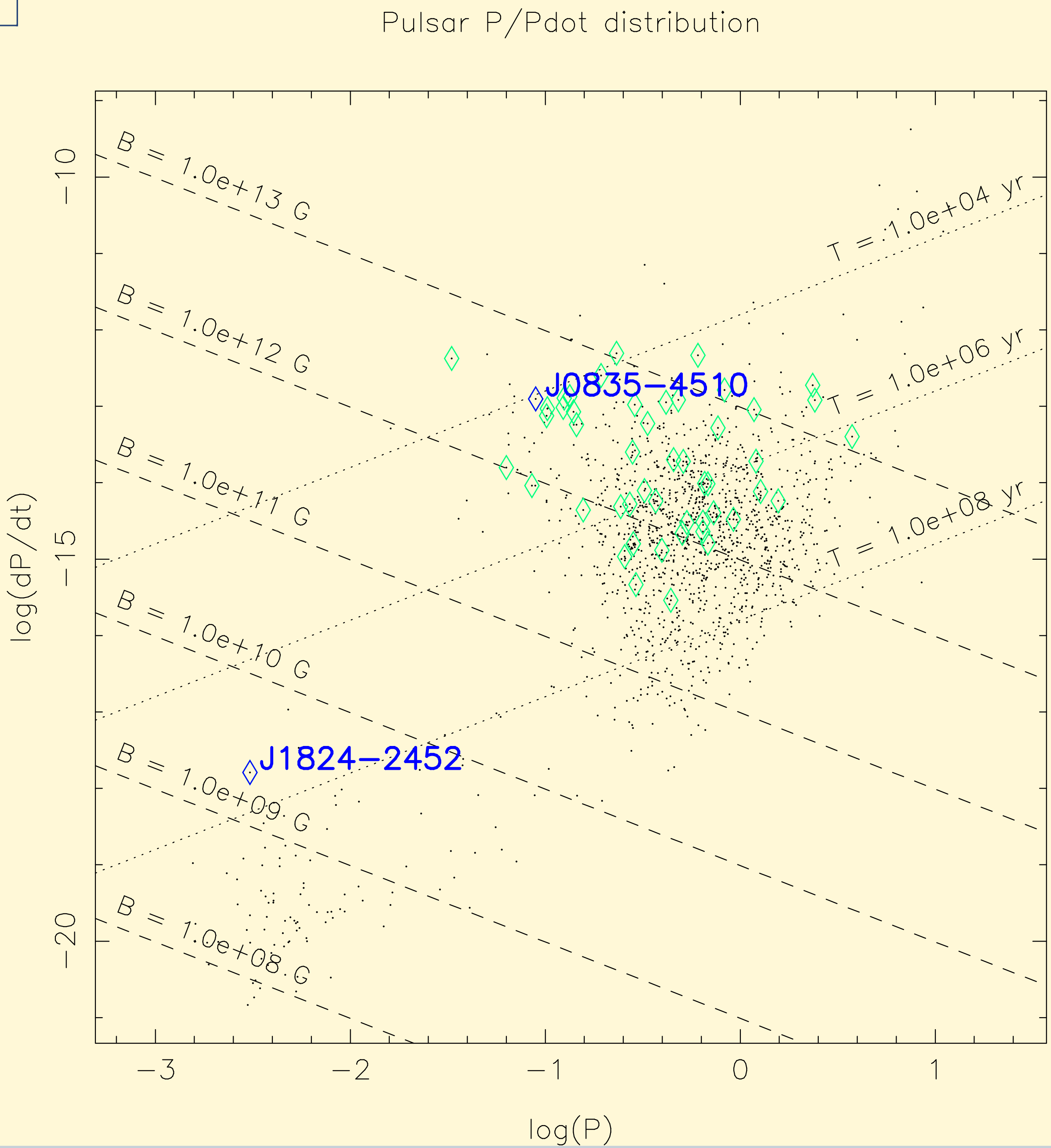

Pulsar $P - \dot{P}$ dot diagram. Pulsars for which one or more glitches have been detected are marked.